International Refrigeration and Air Conditioning Conference

School of Mechanical Engineering

2010

Transient Simulation of Household Refrigerators: A Semi-Empirical, Quasi-Steady Approach

Bruno Borges
Federal University of Santa Catarina

Christian Hermes
Federal University of Parana

Claudio Melo
Federal University of Santa Catarina

Goncalves Goncalves
IFSC

Follow this and additional works at: http://docs.lib.purdue.edu/iracc

Transient Simulation of Household Refrigerators:
A Semi-Empirical, Quasi-Steady Approach

Bruno N. BORGES [1], Christian J. L. HERMES [2*], Joaquim M. GONÇALVES [3], Cláudio MELO [1]

[1] POLO Research Laboratories for Emerging Technologies in Cooling and Thermophysics,
Department of Mechanical Engineering, Federal University of Santa Catarina,
88040-970, Florianópolis, SC, BRAZIL

[2] Department of Mechanical Engineering, Federal University of Paraná,
P.O. Box 19011, 81531-990, Curitiba, PR, BRAZIL

[3] AC&R Center, Federal Institute of Technological Education of Santa Catarina,
88103-310, Rua Jose Lino Kretzer 608, São Jose, SC, BRAZIL

[*] Corresponding Author, Phone: ++55 41 3361 3239, e-mail: chermes@ufpr.br

ABSTRACT

This paper outlines a simplified model to simulate the cycle behavior of household refrigerators and thereby predict their energy consumption. The modeling methodology follows a quasi-steady approach, where the refrigeration system and also the refrigerated compartments are modeled following steady-state and transient approaches, respectively. The model was based on both physical laws and empirical data. The mass, energy and momentum conservation principles were used to compile the equation set, whereas experimental data were collected and applied to derive the model closing parameters, such as the thermal conductance of the heat exchangers and the thermal capacitance of the refrigerated compartment. The experiments were carried out using a controlled temperature and humidity environmental chamber. The model predictions were compared to experimental data taken at ambient temperatures of 25 and 32°C. It was found that the energy consumption is well predicted by the model with a maximum deviation of ±2%. A sensitivity analysis was also carried out to explore the effects of the component characteristics on the product energy consumption and also to identify opportunities for energy savings.

1. INTRODUCTION

Governments worldwide are continually launching ever more stringent energy consumption policies for household refrigerators and freezers. In order to fulfill the new energy regulations most manufacturers are seeking alternative ways to improve the thermodynamic performance of their products. In general, the design and analysis of household refrigerators follow a trial-and-error procedure, which is costly and time consuming. There is considerable evidence in the literature (Gonçalves and Melo, 2004; Hermes and Melo, 2006; Knabben *et al*., 2008) that numerical simulation and optimization techniques can be used to reduce not only the amount of tests and prototypes needed during the product development phase, but also the final product cost and energy consumption. Many different modeling strategies are available in the literature, although most of them have limitations either in terms of physical modeling or computational performance.

In a previous study, Gonçalves and Melo (2004) investigated the steady-state behavior of a top-mount refrigerator by measuring and modeling the performance characteristics of each of its components. The models were based on first principles and also on empirical data. Measurements of the relevant variables were taken at several positions along the refrigeration loop, generating performance data not only for the whole unit but also for each of the cycle components. The experiments were planned and performed following a statistical methodology and considering 13 independent variables that led to over 160 data runs. The model predictions for cooling capacity and power

consumption were compared with experimental data and a maximum deviation of ±10% was found. Such an approach, however, is not suitable for predicting the energy consumption of household refrigerators due to its steady-state nature. In order to overcome this limitation Hermes and Melo (2006) introduced a first-principles model for simulating the transient behavior of household refrigerators and freezers. The model was used to simulate a typical top-mount refrigerator, where the compressor is on-off controlled by the freezer temperature, while a thermo-mechanical damper is used to set the fresh-food compartment temperature. Numerical predictions were compared to experimental data, and it was found that the energy consumption was reasonable well predicted by the model with maximum disagreement within a ±10% band. The compartment air temperatures were also well predicted by the model with a maximum deviation of ±1°C. Such a model, however, requires a considerable amount of CPU time, not being viable for optimization tasks that may require thousands of runs in a row.

In order to address these drawbacks, Knabben *et al.* (2008) proposed a simplified methodology to predict the energy consumption of household refrigerators and freezers with a similar accuracy, but with a substantially lower CPU effort than that required by the dynamic simulation code of Hermes and Melo (2006). The model follows the steady-state, semi-empirical approach introduced by Gonçalves and Melo (2004), but it is able to predict the refrigerator runtime as a function of the cabinet thermal load and cooling capacity ratio. This methodology satisfactorily predicts the energy consumption of refrigerators with fan-supplied heat exchangers, but its applicability to refrigerators with natural draft heat exchangers is still under discussion. Furthermore, it is not able to take into account the impact of events such as door openings, defrost strategy and internal loads on the energy consumption. Such findings have motivated the development of a novel, but still simplified, modeling approach, according to which the refrigeration system and the refrigerated compartments are modeled in steady-state and transient modes, respectively. It should be emphasized that the semi-empirical nature of the approach described by Knabben *et al.* (2008) was retained as the model closing parameters were derived from experimental data.

2. MATHEMATICAL MODEL

The mathematical modeling approach follows that introduced by Knabben *et al.* (2008), according to which the refrigeration loop is divided into the following lumped sub-models: compressor, evaporator, condenser, and internal heat exchanger, as depicted in Fig. 1. In addition, an algebraic transient model was devised for the refrigerated compartments based on the work of Hermes and Melo (2006), to predict the time evolution of the compartment temperatures.
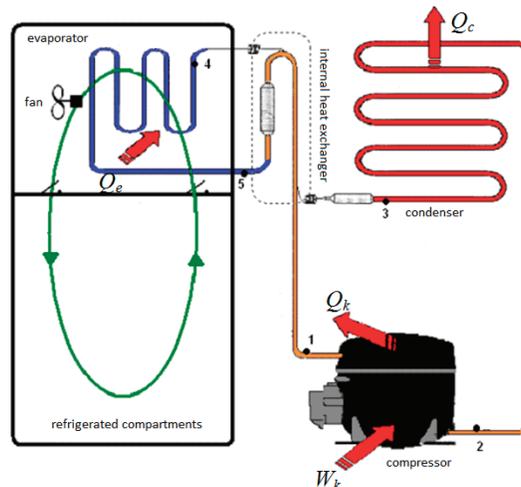

Figure 1. Schematic representation of the refrigerator

2.1 Refrigeration loop sub-model (steady-state)
The compressor sub-model provides not only the compression power but also the refrigerant mass flow rate and the refrigerant enthalpy at the compressor outlet. The refrigerant mass flow rate, m_r, was derived from equation (1), where η_v stands for the compressor volumetric efficiency.

$$m_r = \eta_v V_k N / v_1 \tag{1}$$

The compression power, W_k, was obtained from equation (2), where η_g stands for the compressor overall efficiency.

$$W_k = m_r \left(h_{2,s} - h_1 \right) / \eta_g \tag{2}$$

The refrigerant enthalpy at the compressor outlet, h_2, was calculated from an energy balance at the compressor shell, as follows:

$$h_2 = h_1 + \left(W_k - Q_k \right) / m_r \tag{3}$$

The compressor heat release rate to the surroundings, Q_k, was calculated from

$$Q_k = UA_k \left(T_{2,s} - T_a \right) \tag{4}$$

where T_a is the ambient temperature, $T_{2,s}$ is the isentropic compressor discharge temperature, and UA_k is the compressor shell thermal conductance.

The refrigerant enthalpy at the entrance of the evaporator and the refrigerant temperature at the compressor inlet are calculated from an energy balance involving the internal heat exchanger, as follows:

$$h_4 = h_3 + h_5 - h_1 \tag{5}$$
$$T_1 = T_5 + \varepsilon_x \left(T_3 - T_5 \right) \tag{6}$$

The condenser and evaporator sub-models provide not only the refrigerant enthalpies and air temperatures at their respective outlets, but also the heat transfer rates. The evaporator cooling capacity, the refrigerant enthalpy and the air temperature at the evaporator outlet were calculated respectively as

$$Q_e = m_a c_{p,a} \left(T_{i,e} - T_e \right) \left[1 - exp \left(-UA_e / m_a c_{p,a} \right) \right] \tag{7}$$
$$h_5 = h_4 + Q_e / m_r \tag{8}$$
$$T_{o,e} = T_{i,e} + Q_e / m_a c_{p,a} \tag{9}$$

where $T_{i,e}$ is the air temperature at the evaporator inlet and T_e is the evaporating temperature. Similarly, assuming that the condenser subcooling region occupies only a small part of the condenser and also that the heat flux at the superheating region is of the same order as that observed in the two-phase region, the condenser heat transfer rate and the refrigerant enthalpy at the condenser outlet were calculated, respectively, from

$$Q_c = UA_c \left(T_c - T_a \right) \tag{10}$$
$$h_3 = h_2 - Q_c / m_r \tag{11}$$

The condensing and evaporating pressures were calculated as suggested by Knabben et al. (2008),

$$p_c = p_{sat} \left(T_3 + \Delta T_{sub} \right) \tag{12}$$
$$p_e = p_{sat} \left(T_5 - \Delta T_{sup} \right) \tag{13}$$

where the refrigerant superheating at the evaporator outlet and the refrigerant subcooling at the condenser inlet were taken as input data. It should be noted that the compressor volumetric and overall efficiencies η_v (=0.576–0.0162 p_c/p_e) and η_g (=0.860–0.00459 p_c/p_e), were obtained from the manufacturer's catalogue. All other empirical parameters (UA_k, UA_e, UA_c, and ε_x) were derived from experimental tests carried out with the refrigerator under analysis.

2.2 Sub-model (transient) for refrigerated compartments

The cabinet sub-model calculates the evolution of the temperatures of the refrigerated compartments over time, and also the air temperature at the evaporator inlet. The time evolution of the air temperature inside each refrigerated compartment is described by the following ordinary differential equation (ODE),

$$C_* \dot{T}_* = \left(UA_* + \Phi_* \right) \left(T_a - T_* \right) \pm UA_m \left(T_r - T_f \right) + m_* c_p \left(T_{o,e} - T_* \right) + \sum W_* \tag{14}$$

where the asterisk stands for the frozen-food, T_f, or the fresh-food, T_r, compartment temperature. The "±" signal applies to the frozen-food and the "−" signal to the fresh-food compartment. The air flow rates are calculated from

$$m_f = rm_a \tag{15}$$

$$m_r = (1-r)m_a \tag{16}$$

where r is the air mass fraction supplied to the frozen-food compartment. The thermal capacities, C_*, the thermal conductances, UA_*, and the correction factors, Φ_*, were all derived from experimental tests carried out with the refrigerator under analysis. The Φ-factor was introduced to account for variations in the thermal conductances, since the values supplied to the model were obtained under steady-state conditions.

Furthermore, assuming that the empirical coefficients do not vary over a time-step, Δt, equation (14) can be solved analytically, yielding

$$T_* = T_{eq,*} - \left(T_{eq,*} - T_*^\circ\right)exp\left(-A_*\Delta t/C_*\right) \tag{17}$$

where $T_{eq,*}$ and A_* are given in Table 1 for the 'on' and 'off' operation regimes. Equation (17) provides the temperature variation over a time interval Δt based on the temperatures at the end of the previous time-step. The boundary condition of the evaporator sub-model is calculated at each time-step as follows:

$$T_{i,e} = (1-r)T_r + rT_f \tag{18}$$

Table 1. Terms of equation (17) for the 'on' and 'off' operation regimes

Compartment	ON	OFF
Frozen-food	$T_{eq,f} = \dfrac{UA_f T_a + UA_m T_r + rm_a c_{p,a} T_{o,e} + W_v}{UA_f + UA_m + rm_a c_{p,a}}$	$T_{eq,f} = \dfrac{(UA_f + \Phi_f)T_a + UA_m T_r}{UA_f + UA_m + \Phi_f}$
	$A_f = UA_f + UA_m + rm_a c_{p,Pa}$	$A_f = UA_f + UA_m + \Phi_f$
Fresh-food	$T_{eq,r} = \dfrac{UA_r T_a + UA_m T_f + (1-r)m_a c_{p,a} T_{o,e}}{UA_r + UA_m + (1-r)m_a c_{p,a}}$	$T_{eq,r} = \dfrac{(UA_r + \Phi_r)T_a + UA_m T_f}{UA_r + UA_m + \Phi_r}$
	$A_r = UA_r + UA_m + (1-r)m_a c_{p,a}$	$A_r = UA_r + UA_m + \Phi_r$

2.3 Numerical scheme

The solution algorithm is illustrated in the information flow diagram depicted in Fig. 2. When the simulation starts it is assumed that the refrigerator is switched off. The temperature rise in each compartment is calculated through equation (17) until the thermostat start-up temperature is reached. Thus, the refrigeration loop sub-model is activated and its equations are simultaneously solved at each time-step via the Newton-Raphson method. The calculation takes place until the thermostat cut-off temperature is reached. This procedure is repeated for ten complete cycles, the last three being used to integrate the energy consumption. Each simulation run took approximately 5 minutes to be completed with a 2.66 GHz Intel® Core™ 2 QUAD processor. The code was implemented using the EES (Klein, 2002) and the REFPROP7 (Lemmon *et al.*, 2002) platforms.

3. EXPERIMENTAL WORK

3.1 Experimental apparatus

The system under analysis is a top-mount frost-free refrigerator with a 110-liter frozen-food compartment and a 330-liter fresh-food compartment running with 100g of HFC-134a. The frozen-food compartment temperature is controlled by a thermostat that switches the compressor on and off, whereas the fresh-food compartment temperature is controlled by a thermostatic damper that varies the supplied air flow rate. The system is comprised of a 60 Hz, 6.76 cm³ reciprocating compressor, a natural draft wire-and-tube condenser and a finned-tube 'no-frost' evaporator. The refrigerator was instrumented and positioned inside an environmental chamber with controlled air temperature and humidity. T-type thermocouples were installed at the compressor suction and discharge ports and at the condenser inlet and outlet sections. Pressure transducers were also installed at the compressor suction and discharge ports. The freezer and fresh-food compartment temperatures were measured by three thermocouples appropriately distributed inside the compartments. The air temperature at the evaporator inlet and outlet ports was

also measured. The power consumptions of the compressor and the evaporator and condenser fans were also monitored. Tests were carried out before and after the instrumentation process to check for any effect on the system performance.
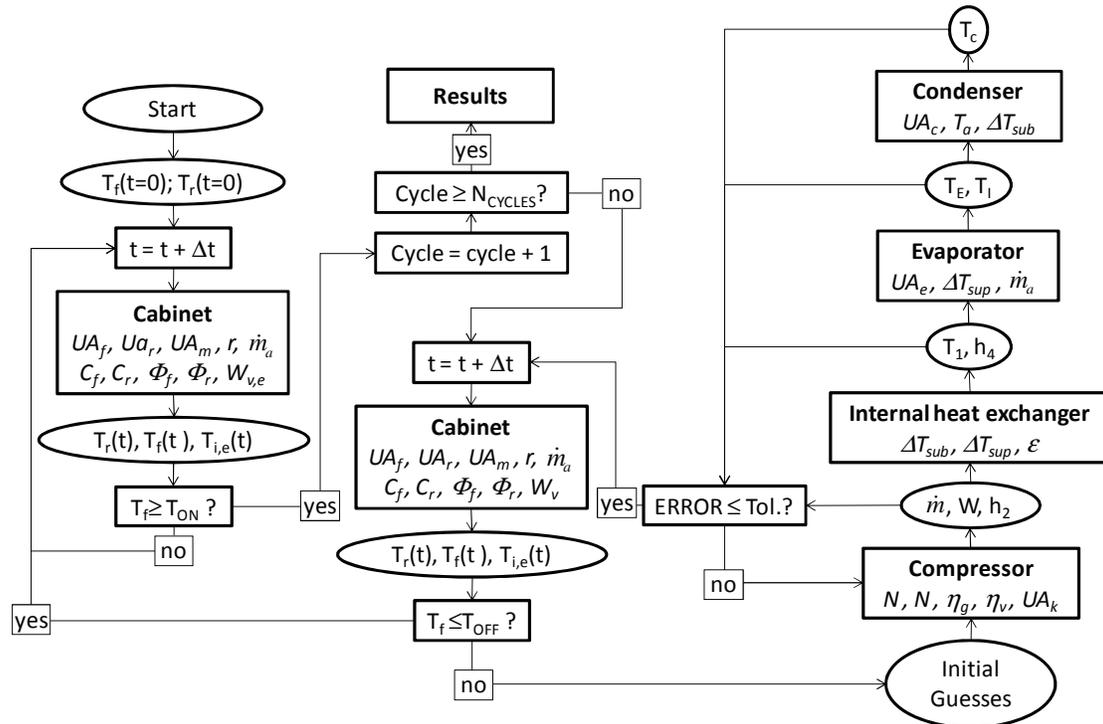

Figure 2. Information flow diagram of the calculation procedure

3.2 Experimental tests

Firstly, steady-state tests were carried out at the ambient temperatures of 25 and 32°C in order to generate the data needed to derive the cabinet thermal conductances (UA_r and UA_f). To this end, electrical heaters were placed inside the refrigerated compartments to balance the cooling capacity and thereby keep the compartment temperatures at the desired levels. Secondly, energy consumption tests were carried out following the ANSI/AHAM HRF-1 (2004) standard at the ambient temperatures of 25 and 32°C, not only to collect data required to derive the other empirical parameters (UA_k, UA_c, UA_e, ε_x, r, Φ_f, Φ_r, C_f, C_r, ΔT_{sub}, ΔT_{sup}, T_{on} and T_{off}) but also for the model validation exercise. The empirical parameters were obtained by supplying the model with experimental data on the temperatures and power consumption. The results thus obtained are summarized in the Appendix. It should be noted that the Φ-factor is almost nil for the frozen-food compartment whereas it has a significant effect on the fresh-food compartment, since the latter is more sensitive to the compressor and condenser heat loads.

4. RESULTS AND DISCUSSION

4.1 Model validation

The model results were compared to the energy consumption data obtained at 25 and 32°C, as summarized in Table 2. It can be seen that the model predictions for the energy consumption and runtime ratio are quite good, with maximum discrepancies of ±2%. Moreover, the refrigerated compartment temperatures are well predicted by the model, with a maximum deviation of ±0.4ºC. Figure 3 shows the compressor power consumption while Fig. 4 shows the compartment temperatures during three cycles, at an ambient temperature of 32ºC. Once again it is evident that the model predictions are very close to the experimental data. It should be mentioned that the difference between the calculated and measured cycles is due to the runtime ratio prediction error which accumulates over time.

4.2 Parametric analysis

A sensitivity analysis to assess the influence of specific design parameters on the overall energy consumption at an ambient temperature of 32ºC was also carried out. The effect of the evaporator and condenser thermal conductances

on the system performance is shown in Figures 5 and 6, respectively. As expected (Hermes and Melo, 2006, Knabben *et al*., 2008), the energy consumption decreases asymptotically as the thermal conductance increases. This occurs because from a certain point the impact of the thermal conductance on the temperature difference between the air and refrigerant stream becomes imperceptible and likewise the energy savings. It can also be seen that for this particular product the condenser shows more room for improvement than the evaporator.

Table 2. Comparison between model predictions and experimental data

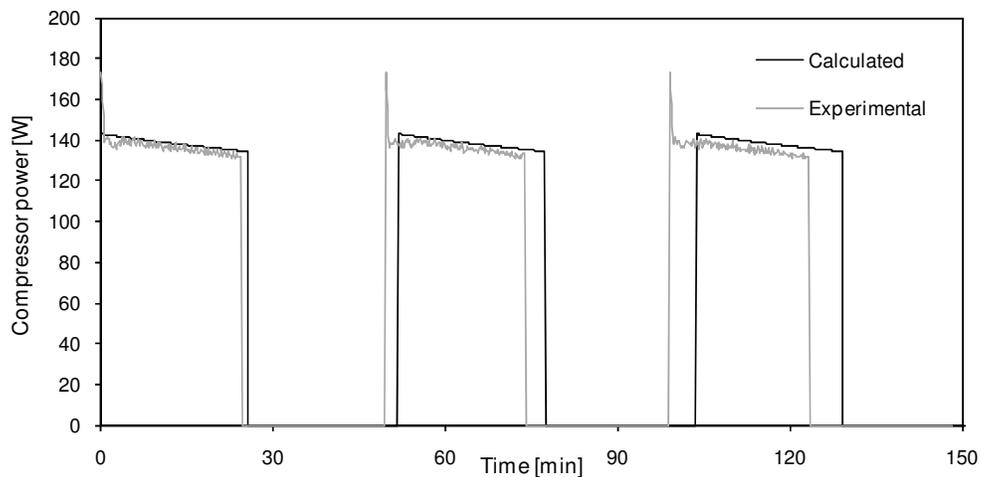| Parameter	T_a=25°C			T_a=32°C		
	Exp.	Calc.	Diff.	Exp.	Calc.	Diff.
Energy consumption [kWh/month]	35.0	35.4	1.3%	48.8	49.4	1.2%
Runtime ratio [dimensionless]	0.372	0.378	1.8%	0.496	0.495	-0.1%
Frozen-food temperature [°C]	-17.7	-17.6	0.1	17.9	-18.0	-0.1
Fresh-food temperature [°C]	4.9	4.5	-0.4	4.7	4.3	-0.4

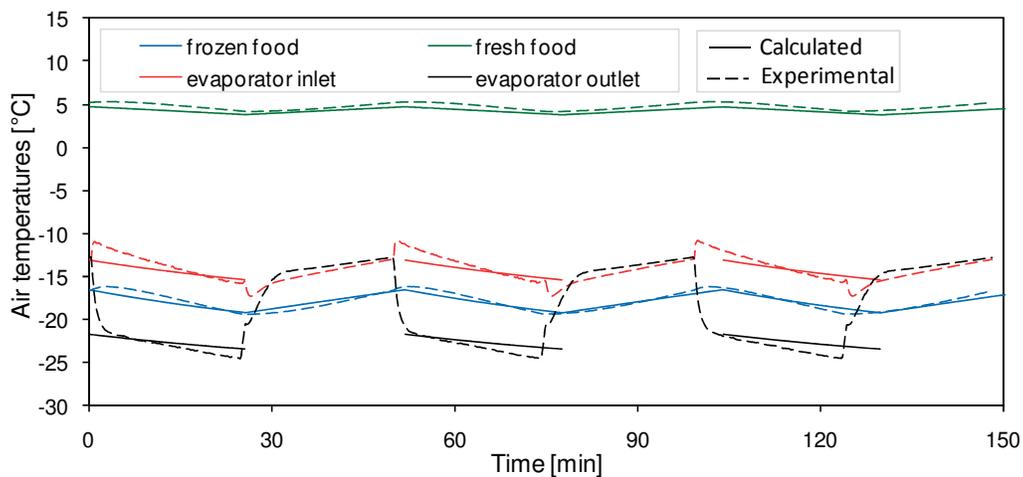Figure 3. Comparison between calculated and measured compressor power

Figure 4. Comparison between calculated and measured compartment temperatures

Figures 7 and 8 show that the energy consumption is almost linearly affected by the thermal conductances of the compartments, as expected. The influence of the thermal capacities on the energy consumption were also

investigated, and it was found that they have a marginal effect on the system performance (this observation being corroborated by results published by Hermes and Melo, 2006).
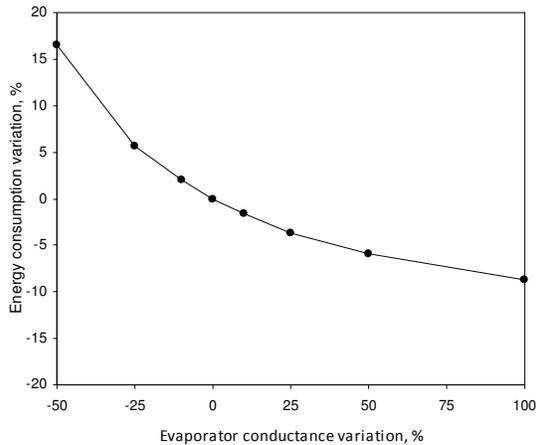

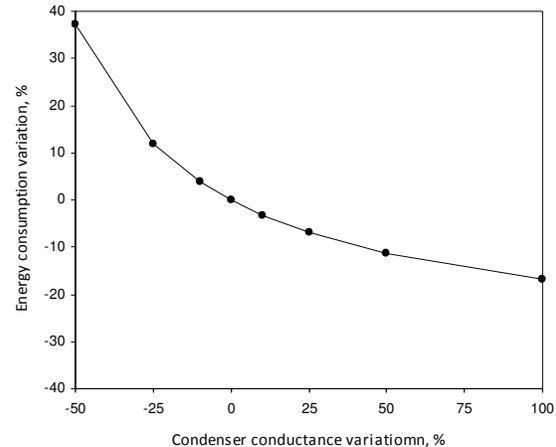Figure 5. Effect of evaporator conductance

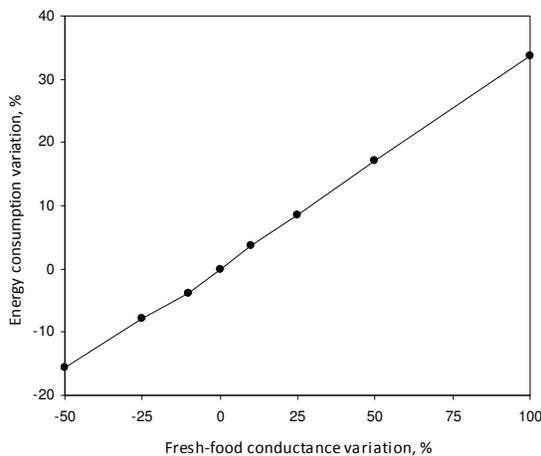Figure 6. Effect of condenser conductance
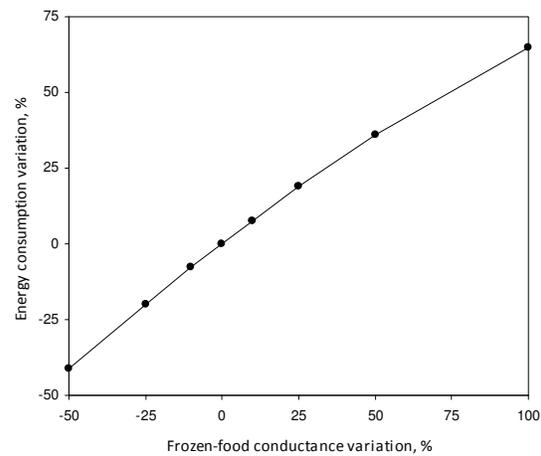

Figure 7. Effect of fresh-food conductance

Figure 8. Effect of frozen-food conductance

5. SUMMARY AND CONCLUSIONS

A simplified quasi-steady methodology for predicting the energy consumption of household refrigerators using a hybrid semi-empirical model (steady-state refrigeration loop and transient refrigerated compartments) was proposed and validated against experimental data. The model predictions were compared with their experimental counterparts, showing a maximum deviation of ±2% for the energy consumption and runtime ratio, and a maximum difference of ±0.4°C for the compartment temperatures. It was also observed that the predicted power consumption and compartment temperatures followed closely the experimental trends during the cycle transients.

The model was also used to assess the energy performance of a top-mount frost-free refrigerator in terms of the evaporator and condenser conductances, the fresh- and frozen-food compartment conductances and thermal capacities. It was shown that the product energy consumption can be reduced by 5% if the evaporator conductance is increased by 40%, the condenser conductance is increased by 20%, the fresh-food conductance is decreased by 10%, or the frozen-food conductance is decreased by 5%. The combined effect of these parameters will be investigated in a further study.

Moreover, the model proposed herein is intended to be applicable to investigations to ascertain the influence of events such as door openings, internal loads and defrost strategies on the energy consumption, which will also be addressed in a future publication. Finally, it should be emphasized that the model requires only 5 minutes of CPU

time (Intel® Core™ 2 QUAD 2.66 GHz processor) to carry out an energy consumption prediction, a value substantially lower than that required by more sophisticated dynamic simulation models.

ACKNOWLEDGEMENTS

REFERENCES

ANSI/AHAM HRF-1, 2004, Energy performance and capacity of household refrigerators, refrigerator-freezers and freezers, American National Standards Institute, Washington-DC, USA.

Gonçalves JM, Melo C, 2004, Experimental and numerical steady-state analysis of a top-mount refrigerator, Int. Refrig. Conf. at Purdue, West Lafayette-IN, USA, Paper R078

Hermes CJL, Melo C, 2006, A dynamic simulation model for fan-and-damper controlled refrigerators, 11th Int. Refrig. Conf. at Purdue, West Lafayette, USA, Paper R036

Klein, S.A., 2009, Engineering Equation Solver, Professional Version 8.413-3D, F-Chart software, Madison-WI.

Knabben, F.T., Hermes, C.J.L., Melo, C., Gonçalves, J.M., 2008, A Simplified Steady-State Model for Predicting the Energy Consumption of Household Refrigerators and Freezers, Int. Refrig. Conf. at Purdue, West Lafayette, USA, Paper 2145

Lemmon E.W., McLinden M.O., Huber M.L., 2002, NIST Reference fluids thermodynamic and transport properties – REFPROP 7.0, National Institute of Standards and Technology, Gaithersburg, MD, USA

NOMENCLATURE

Roman
C, thermal capacity, J/K
c_p, specific heat at constant pressure, J/kgK
h, enthalpy, J/kgK
m, mass flow rate, kg/s
N, compressor speed, Hz
Q, heat transfer rate, W
T, temperature, K
$\dot{T}$, time derivative of temperature, K/s
v, specific volume, m³/kg
V, volume, m³
W, power, W
UA, thermal conductance, W

Greek
Δt, time-step, s

Φ, conductance correction factor, W/K
ε, heat exchanger effectiveness, dimensionless
η, compressor efficiency, dimensionless

Subscripts
a, air, adiabatic process
c, condenser
e, evaporator
i, inlet
k, compressor
m, mullion
o, outlet
f, frozen-food
r, refrigerant, fresh-food
s, isentropic process
x, internal heat exchanger

APPENDIX

Cycle test data
UA_k=1.336 W/K
UA_c=8.51+0.120 T_a, with T_a in [ºC], UA_c in [W/K]
UA_e=12.0+0.266 T_a, with T_a in [ºC], UA_e in [W/K]
ε_x=0.572+0.00434 T_a, with T_a in [ºC]
r=0.894–0.00181 T_a, with T_a in [ºC]
Φ_f=–0.013 W/K
Φ_r=–0.545 W/K
C_f=1.971 10^4 J/K

C_r=6.092 10^4 J/K
ΔT_{sub}=0 ºC
ΔT_{sup}=3 ºC
T_{on}=–15.56–0.0325 T_a, with T_a in [ºC], T_{on} in [ºC]
T_{off}=–16.26–0.0943 T_a, with T_a in [ºC], T_{off} in [ºC]

Steady-state test data
UA_r=1.932 W/K
UA_f=0.635 W/K